© Universiti Tun Hussein Onn Malaysia Publisher's Office

IJIE

http://penerbit.uthm.edu.my/ojs/index.php/ijie
ISSN : 2229-838X e-ISSN : 2600-7916

The International Journal of Integrated Engineering

Glass-Embedded Fan-Out Antenna-in-Packaging for 5G Millimeter Wave Applications

Chia-Hao Liu[1], Ren-Kai Lu[1], Hsien Chung[2*], Ben-Je Lwo[1], Tom Ni[3], Alice Pan[3]

[1]Department of Mechanical and Aerospace Engineering, Chung-Cheng Institute of Technology,
National Defense University, Taoyuan 335, Taiwan, R.O.C.

[2]Weapon System Center, Chung-Cheng Institute of Technology,
National Defense University, Taoyuan 335, Taiwan, R.O.C.

[3]Industrial Internet Semiconductor and Software Business Group,
Hon Hai Technology Group, Hsinchu 300, Taiwan, R.O.C.

*Corresponding Author

DOI: https://doi.org/10.30880/ijie.2022.14.06.019
Received 06 September 2021; Accepted 17 March 2022; Available online 10 November 2022

Abstract: The paper proposes a novel Antenna-in-Packaging (AiP) structure design for 60 GHz, millimeter wave WiFi applications. In the AiP design, single- or double-sided glass redistribution layers were embedded in a typical fan-out (FO) packaging structure to introduce design flexibility and to improve the radiation properties of the antenna. ANSYS-HFSS software was employed for electromagnetic (EM) characteristic simulations on the fan-out AiP (FO_AiP) design. To improve antenna radiation performance, single factor analyses were first performed to study the impact of each of the design parameters. A consecutive procedure followed to find more suitable combinations of the design parameters. As a result, two typical glass-embedded FO_AiP structures - one with 7.6 GHz bandwidth plus 4.7 dB gain and upward radiation, and another with 5.3 GHz bandwidth plus 5.2 dB gain and downward radiation, are proposed for the 60 GHz applications.

Keywords: FOAiP, glass-embedded packaging, millimeter wave, radiation property

1. Introduction

Wireless communication systems are rapidly developing in recent years, and the operation frequencies of mobile consumers and radio frequency (RF), Internet of Things (IoT) devices have continuously increased due to high bandwidth requirements. Consequently, potential WiFi applications of 5G millimeter wave technology at 60 GHz have drawn considerable since IEEE initiated a new standard in 2007 [1]- [2]. Because the wavelength of 5G communication has a millimeter scale, level 1 or the modulus electronic packaging has become a suitable solution for future 5G antenna-in-packaging (AiP) applications [3]- [5]. This is because the packaging dimensions are compatible with the wavelength of an electromagnetic wave. As a result, AiP technologies in which an antenna is integrated into RF chip packaging have been developed to provide a compatible and low loss antenna solution for future devices.

Without a printed circuit board (PCB) or substrate, fan-out packaging extends the routing and interconnecting size through redistribution layers (RDLs). Because of its low structure profile, compact in size, high I/O density, low interconnection loss and good thermal and electrical performance [6]- [7], FO technology is suitable for future AiP devices on 5G IoT or mobile applications. Consequently, solutions using FO_AiP technology for 5G applications have attracted substantial attention over the past three years [8]- [11]. An effective AiP design must incorporate an antenna

---

*Corresponding author:hchung.sean@gmail.com and package-specific characteristics. In the current study, a new glass-embedded FO_AiP structure was proposed for 5G millimeter Wave devices. Since RDLs can be added on a single side or on both sides of the embedded glass, the newly developed structure provides greater design flexibility which may facilitate improvement in the electromagnetic radiation properties of the antenna. To simulate the high-frequency electromagnetic (EM) behavior of new FO_AiP designs, a commercial 3D full-wave simulation software (ANSYS HFSS) was used. After single factor analyses followed by a consecutive procedure for design optimization, availability on several glass-embedded FO_AiP structure designs and their RF performances are finally presented and discussed.

2. The Antenna Structure and The Methodology

Fig. 1 presents the architecture of a slot-coupled patch antenna unit for the glass-embedded FO_AiP. The RF chip signals are interconnected to the feeding line at the back of the antenna unit. Note that an actual AiP design generally includes an antenna unit in an array. According to Tasi, et al. [12], chip overlap in the antenna area reduces the antenna gain; thus, the overlap is not recommended. The dimensions of the structure are approximately 3 mm × 3 mm × 1.8 mm for the antenna unit, and 2.2 mm × 2.5 mm × 0.2 mm for the embedded glass, respectively. Default material properties were used for the simulations in ANSYS-HFSS (High Frequency Structure Simulator). In Fig. 1, RDL-1 (the feeding interconnection and the reflector layer) and RDL-3 (the patch layer) are the RDLs at the top and bottom, respectively, of the molding compound (MC). The grounding coplanar waveguide (CPW) layer and the microstrip for the slot-coupled antenna are located at RDL-2 beneath the glass. Adding the embedded glass improves the design flexibility of the packaging from the traditional FO_AiP structure because additional RDLs can be added on the top and/or bottom (such as RDL-2) of the glass. The advantages of RDLs on glass surfaces are discussed in Section IV with simulated data.

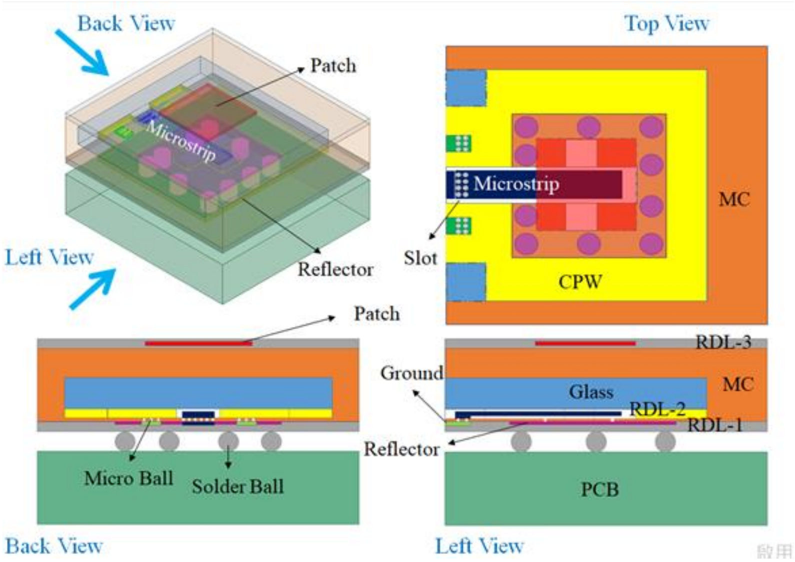

Fig. 1 - Architecture of an antenna unit

To evaluate the antenna performance, the bandwidth was determined based on the return loss S11 = -10 dB, the 60 GHz gain, and the central frequency (CF) of the -10 dB band. A qualified antenna design requires a gain of at least 4.5 dB with a larger bandwidth, and CF of approximately 60 GHz is needed to fulfill the requirements from the antenna applications. To identify the significance and effects of each of the design parameters on the aforementioned mentioned EM characteristics, single factor analyses were first performed to simulate the radiation performance of an antenna unit by fixing each of the original design parameters except one. A consecutive procedure was followed to improve the structure designs in accordance with design parameters combinations. In the procedure, design parameters were individually switched at each step with the best design from the previous step used as a new base for the following step. We finally discussed the performances of two typical FO_AiP designs.

3. The Single Factor Analyses

Fig. 2 contains plots of radiation characteristics for various microstrip lengths and widths. According to the plots, microstrip length was significantly related to the central frequency (CF) and the bandwidth (BW), and microstrip width was a key factor for CF and the antenna gain, respectively. The plots in Fig. 3 present the effects for two slot design parameters. The figures indicated that an antenna with a larger microstrip-CPW spacing was preferred for its higher bandwidth, and an antenna with a smaller slot ear length was preferred for its higher gain and greater bandwidth. As shown in Fig. 3b, a second band with 25-35 GHz of central frequency appeared when the ear length becomes larger than 0.4 mm (as marked) so that multiple CF datapoints were obtained for ear length larger than 0.4 mm. However, the bandwidth and gain at the second band (not shown) were too small for actual applications.

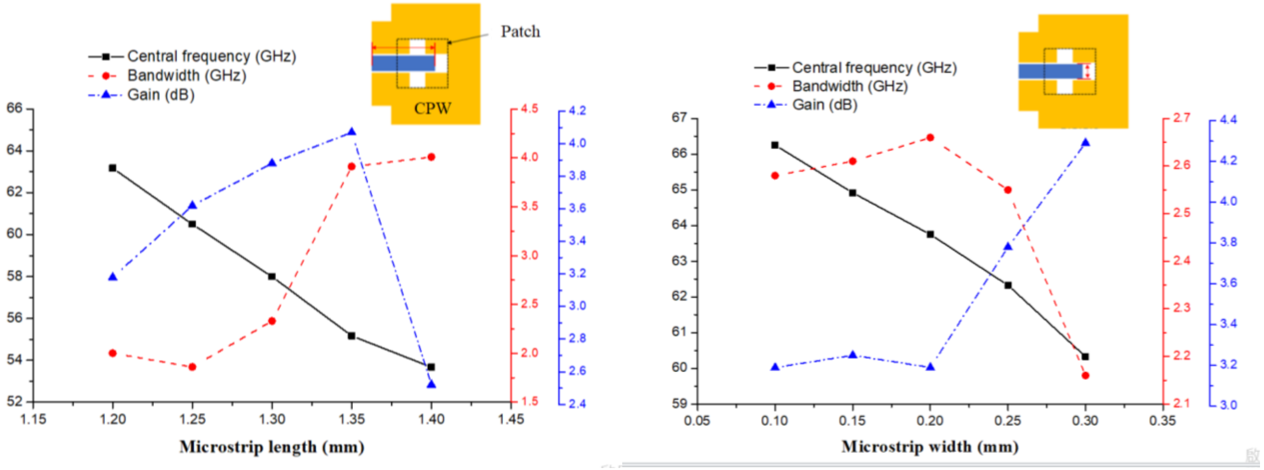

(a) (b)

Fig. 2 - (a) Microstrip length effect; (b) microstrip width effect

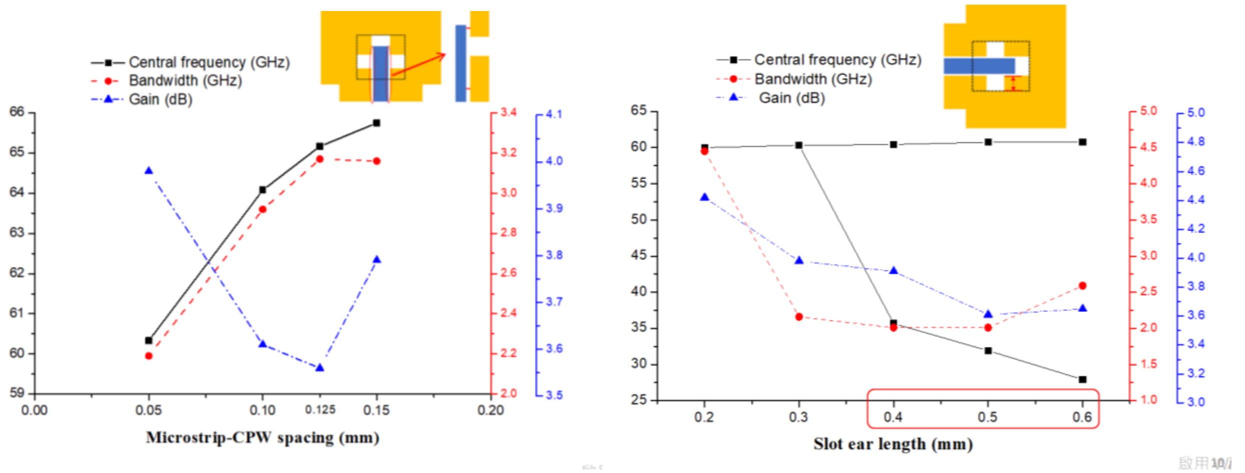

(a) (b)

Fig. 3 - (a) Microstrip-CPW spacing effect, and; (b) slot ear length effect

The effects of the other geometric factors were simulated, and the results are summarized in Table 1. For better illustration of the geometric factors in Table 1, planar presentations of the parameters on the RDL-2 layer, including slot as well as CPW parameters, are depicted in Fig. 4. In addition to the results in Table 1, a floating rectangular ring around the top patch as proposed in [13] was simulated, and the results indicated limited improvement in antenna gain.

In addition to the geometric parameters in Table 1, single factor studies on different structure design parameters were next performed. The relatively important results are summarized as follows:

- Antenna gain was significantly improved by removing solder balls under the AiP unit, but CF and bandwidth were unaffected.
- Moving the patch to the glass top reduced antenna gain, but CF and bandwidth were unaffected.
- Adding a second patch on the glass top to construct a double-patch structure slightly increased CF, but the gain and bandwidth were unaffected.
- Antenna gain for the double-patch structure was significantly improved if a rectangular aperture, which was perpendicular to the microstrip, was added at the center of the lower patch on the glass top surface. In addition, the aperture design improved the bandwidth of the antenna.

Table 1 - EM effects of geometric factors

Factor	**Effect**		
(as presented in Fig. 4)	**CF**	**BW**	**Gain**
Microstrip Length (a)	⇩⇩	⇧⇧	⇧
Microstrip Width (b)	⇩	N	⇧
Microstrip-CPW Spacing (c)	⇧	⇧	N
Slot Ear Length (d)	N	⇩	⇩
Stub Length (e)	⇩	N	⇧
Slot Top Spacing (f)	⇧	⇧	N
Patch Length (g)	N	N	⇧
Patch Width	N	N	N
Glass Thickness	N	N	⇧
MC Thickness	N	⇧	⇧
Antenna Unit Length (h)	N	⇧	⇩⇩
Antenna Unit Width	N	N	⇩

CF: Central Frequency
BW: Bandwidth
⇧⇧/⇩⇩: Significantly increase/ decrease as the factor is increased
⇧/⇩: Increase/ decrease as the factor is increased
N: No Trend

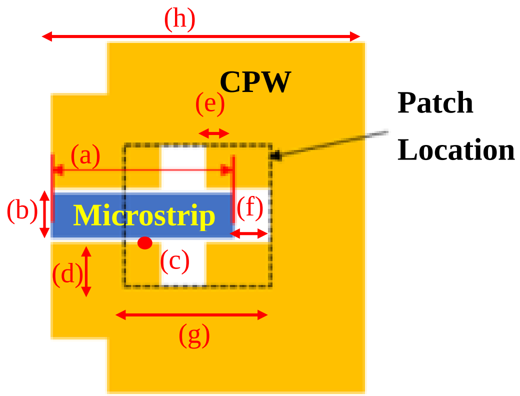

Fig. 4 - Planar presentations of the RDL-2 layer

Note that the final three design items were available in the new proposed antenna design because a second patch can be added on the top surface of the embedded glass; thus, antenna performances could be improved due to the new design flexibility.

4. The Antenna Design Procedure

Based on the results of single factor analyses, a procedure to optimize antenna design was performed. In the design procedure, we first adjusted the microstrip length to obtain a base structure with a CF of approximately 60 GHz. Then, one design parameter was switched at each step (as presented in Fig. 5). At each step, antenna performance was compared with simulation results for five designs including the current base structure, and the most suitable one of the five results was selected as a new base structure for the next step. The procedure was straightforward but tedious, with copious simulated data. Therefore, we present only typical and optimal structures herein for simplicity.

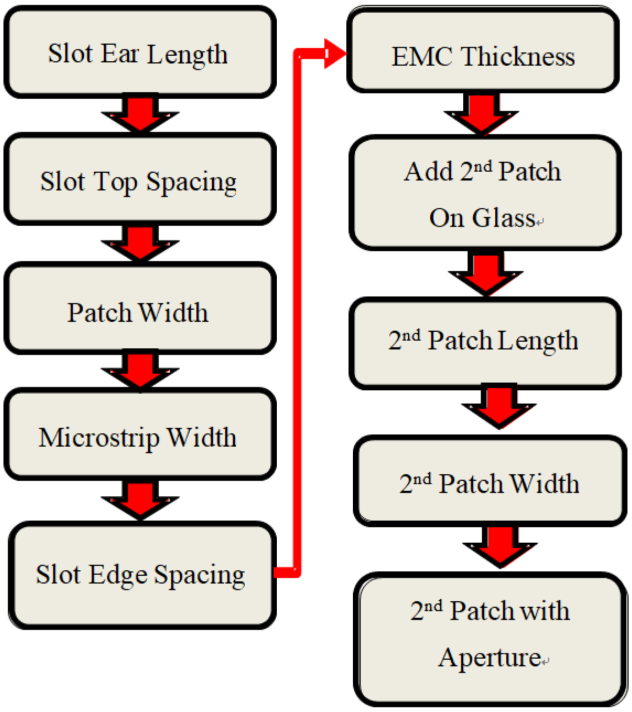

Fig. 5 - Antenna design procedure

In the procedure, antenna performances were continuously improved but the antenna gain did not satisfy the 4.5 dB criteria until a second patch was added onto the top glass surface. To simulate the second patch width according to the procedure in Fig. 5, antennas performances is compared between various second patch width (Fig. 6). It is observed in Fig. 6 that the best antenna structure has a second patch width of 0.8 mm, and the antenna had a 4.7 dB gain with a 7.6 GHz bandwidth. The CF for the structure was 60.5 GHz. Furthermore, as the patch and the CPW are in the horizontal x-y plane, the radiation pattern as presented by the color contour in Fig. 7 was upward because the maximum gain in red color points upward (positive z) to the antenna unit.

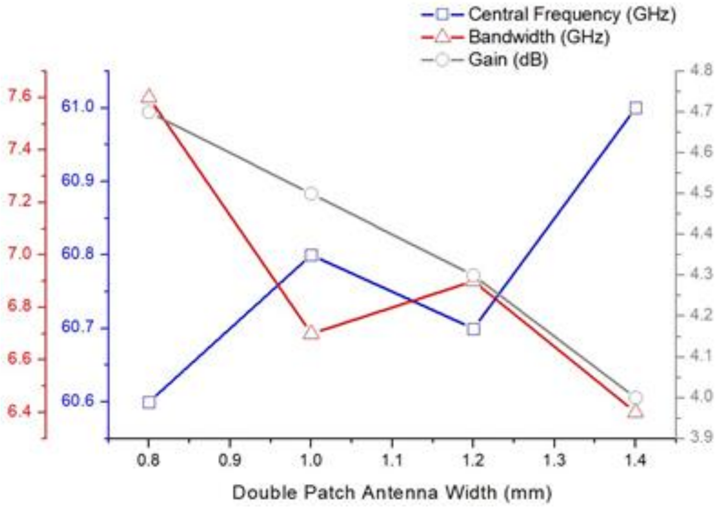

Fig. 6 - Results of the second patch width simulations

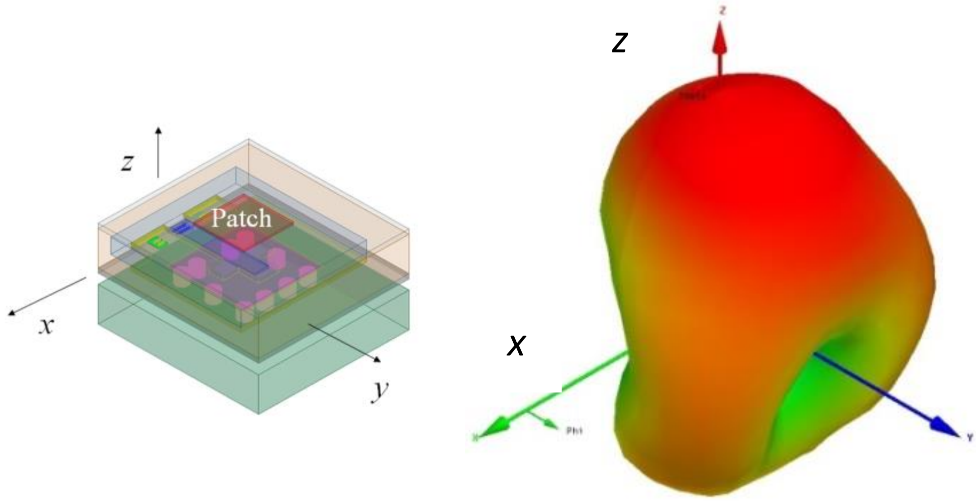

Fig. 7 - Coordinate system and the radiation pattern for the antenna unit with a second patch width of 0.8 mm

After investigating the second patch width, the procedure continued on the second patch with aperture. Finally, the antenna with the optimal performance was obtained from the structure with an aperture on the second patch on the top glass surface, and the radiated EM wave was oriented downward (negative z) as presented in Fig. 8. In this structure, the aperture was perpendicular to the microstrip, and the antenna gain was 5.2 dB. Furthermore, the bandwidth of the antenna was 5.3 GHz (57.6–62.9 GHz) with a CF of 60.2 GHz. Consequently, the aperture significantly increased the antenna gain but altered the radiation pattern, and the bandwidth of the antenna was reduced.

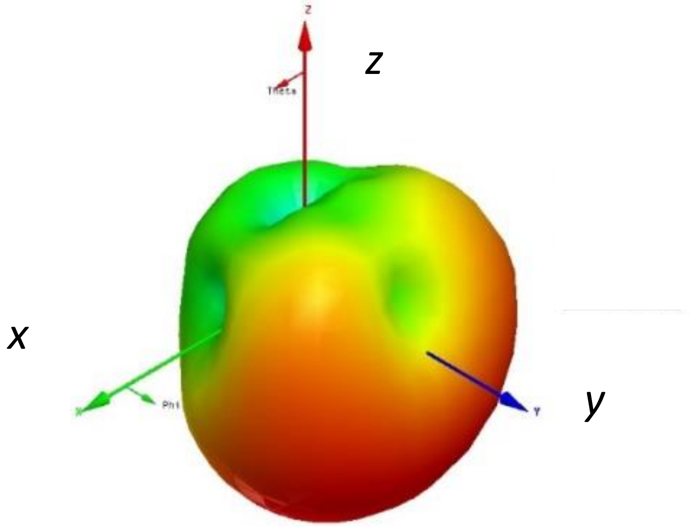

Fig. 8 - Radiation pattern for a double-patch antenna with aperture

5. Conclusion

This paper proposes a new FO AiP structure with a slot-coupled patch design for 60 GHz WiFi applications. Due to the embedded glass, the design flexibility between various second patch width of the antenna structure was improved by the best patch of 0.8 mm made by RDLs on the embedded glass surfaces. After conducting single factor analyses and design optimization procedure through 3D electromagnetic simulations, the final FO_AiP had a bandwidth of up to 7.6 GHz, and the aperture was perpendicular to the microstrip improved the antenna gain of up to 5.2 dB; the radiation pattern could be either upward or downward.

Acknowledgment

The authors fully acknowledged National Defense University and Hon Hai Technology Group for supporting this work.

References

[1] Nitsche, T. *et al*., “IEEE 802.11ad: Directional 60 GHz Communication for Multi-Gigabit-per- Second Wi-Fi,” IEEE Commun. Mag., vol. 52, no. 12, Dec. 2014, pp. 132–141.

[2] Ghasempour, Y. *et al*., “IEEE 802.11ay: Next-Generation 60 GHz Communication for 100 Gb/s Wi-Fi,” IEEE Communications Magazine 55.12 (2017): 186-192.

[3] Wan, W., *et al*. “Wideband Low-profile AMC-based Patch Antenna for 5G Antenna-in-package Application,” 2020 IEEE 70th Electronic Components and Technology Conference (ECTC). IEEE, 2020.

[4] Tsai, M., *et al*. “Advanced Antenna Integration of 3D System in Package Solutions for IoT and 5G Application,” 2019 22nd European Microelectronics and Packaging Conference & Exhibition (EMPC). IEEE, 2019.

[5] Zhang, Y. & Mao, J., “An overview of the development of antenna-in-package technology for highly integrated wireless devices,” Proceedings of the IEEE 107.11 (2019): 2265-2280.

[6] Liu, H.-W., *et al*., “Warpage Characterization of Panel Fan-out (P-FO) Package,” 2014 IEEE ECTC, pp. 1750-1754, 2014.

[7] Rao, V. S., Chong, C. T., *et al*., “Development of High Density Fan Out Level Package (HD FOWLP) with Multi-Layer Fine Pitch RDL for Mobile Application,” 2016 IEEE ECTC, pp. 1522-1529, 2016.

[8] Wang, C. T., Hsieh, J. S., Tsai, J. S., Liu, M., & Yu, C. H., “Integrated Fan Out Antenna and Method of Forming the Same,” United States Patent, US 9,843,106 B2, 2017.

[9] Wang, C.-T., *et al*. "InFO_AiP technology for high performance and compact 5G millimeter wave system integration," 2018 IEEE 68th Electronic Components and Technology Conference (ECTC). IEEE, 2018.

[10] Hsieh, S.-C., *et al*. "mmWave Antenna Design in Advanced Fan-Out Technology for 5G Application," 2019 22nd European Microelectronics and Packaging Conference & Exhibition (EMPC). IEEE, 2019.

[11] Le, T. H., *et al*. "Dual-Band 5G Antenna Array in Fan-Out Wafer-Level Packaging (FOWLP) Technology," 2020 23rd International Microwave and Radar Conference (MIKON). IEEE, 2020.

[12] Tsai, C. H., *et al*., “Array Antenna Integrated Fan-out Wafer Level Packaging (InFO-WLP) for Millimeter Wave System Applications,” 2013 IEEE International Electron Devices Meeting, Washington, DC, USA, pp. 25.1.1-25.1.4, 2013.

[13] Zhang, T., Li, L., Xia, H., Ma, X., & Cui, T. J., “A Low-Cost and High-Gain 60-GHz Differential Phased Array Antenna in PCB Process,” in IEEE Transactions on Components, Packaging and Manufacturing Technology, vol. 8, no. 7, pp. 1281-1291, 2018.